Proceedings Paper:

White Rose
university consortium
Universities of Leeds, Sheffield & York

PWM-based Flux linkage estimation for permanent magnet synchronous machines

Shuai Xiao[1] ✉, Antonio Griffo[1]

[1]*Department of Electronic and Electrical Engineering, The University of Sheffield, Sheffield, UK*
✉ *E-mail: sxiao7@sheffield.ac.uk*

Abstract: Monitoring of rotor temperature in permanent magnet synchronous machines (PMSM) is of great importance as high temperature could cause partial or even irreversible demagnetisation of the permanent magnets (PMs). Rotor temperature measurement unfortunately is particularly difficult in practice, since it is difficult to access temperature sensors on a rotating shaft. Nevertheless, rotor temperature can be obtained indirectly with the information of rotor magnet flux linkage, as PM remanence decreases with rotor temperature. Here, a simple and relatively accurate method for online estimation of PM flux linkage is presented, based on the measurement of current response to the standard space-vector pulse width modulation (SV-PWM). This method uses the already-existing PWM voltage as the excitation signal in order to avoid any form of signal injection which produces undesirable disturbance to the system. Knowledge of machine parameters, such as inductances which may vary due to saturation, is not required. The proposed methodology has been verified in real-time simulation.

1 Introduction

Permanent magnet synchronous machines (PMSMs) are widely popular in servo and traction applications due to their high torque and power density. Their use in applications where high reliability must be guaranteed requires careful online condition monitoring of the motor [1]. Thermal monitoring of the machine is particularly important, since temperature is typically the main environmental stressor causing state-of-health degradation and ultimately failure. In terms of motor stators, several direct and indirect temperature monitoring techniques are well established. Temperature sensors such as thermistors and thermocouples can be relatively easily embedded into machine stators during the manufacturing process. However, the requirement for additional sensors may increase costs. Rotor temperature monitoring is of equal importance as high temperature increases the risk of partial, or even total irreversible demagnetisation of rotor magnets [2]. Rotor temperatures are difficult to measure in practice, as the rotating part can only be accessed through slip rings, infrared or other wireless sensors, making direct measurement unrealistic in some applications. Hence model-based methods, have been investigated in recent years.

One of the most contemporary approaches is thermal-modelling, which is usually based on a lumped parameter equivalent thermal network (LPTN). It can inform a thermal 'observer', which combined with loss models, is capable of providing accurate temperature estimation during real-time operation. Low-order LPTNs [1, 3, 4] in particular have aroused more attention, as the detailed knowledge of the motor internal topology, materials and dimensions is not required. Accurate temperature estimation can be achieved using a measurement-based parameter identification procedure, which continuously updates the values of the thermal parameters based on the minimisation of a specified cost function.

Furthermore, it is also possible to determine motor temperatures via temperature-dependent machine parameters. The use of rotor flux linkage model-based observer is proposed in [2–5] using the fact that (NeFeB) PM loses 0.11–0.12% remanence per one degree Celsius temperature rise. Nevertheless, this method is difficult to apply practically, because of the necessity of a precise modelling for motor and inverter — the model-related errors otherwise will be misinterpreted as temperature changes.

PM temperature can also be potentially acquired indirectly from estimation of the rotor magnet flux linkage. Few estimation methods of PM flux linkage have been presented in publications. [6] proposes an online method to estimate stator resistance and rotor PM flux linkage under constant load torque with two sets of *dq*-axis voltage equations corresponding to $i_d = 0$ and the injection of a $i_d \neq 0$ test signal. Likewise, by utilising a zero-voltage injection scheme, flux linkage is directly determined with the measurement of the average value of the voltage commands which are the output of current loop PI controllers of the standard field-oriented control at different rotor speed [7]. In both methods, the *dq*-axis inductance terms are cancelled during the derivation of the methods, resulting in a parameter-independent estimation. However, signal injection-related methods are not desirable because the additional signal disturbs the motor performance by producing additional current and thus additional torque ripples and additional losses.

Here, a relatively simple and accurate method is presented for online flux linkage estimation, which only involves in the measurements of voltage references and current in response to the standard SV-PWM. Similarly to [6, 7], knowledge of inductances is not required for the estimation. Furthermore, this method does not need signal injection as the excitation signal is intrinsic in the PWM voltage.

After introducing the basics of the method in Section 2, a comprehensive validation is conducted on an interior PMSM (IPMSM) model in real-time, using the hardware-in-the-loop (HIL) technique. The estimation errors in different operating conditions are evaluated and shown to be relatively small.

2 Fundamental theory

The voltage equations of a PMSM represented in rotating *dq*-reference frame are expressed as:

$$v_d = R_s i_d + L_d \frac{\mathrm{d}}{\mathrm{d}t} i_d - \omega_r L_q i_q \tag{1}$$

$$v_q = R_s i_q + L_q \frac{\mathrm{d}}{\mathrm{d}t} i_q - \omega_r (L_d i_d + \psi_m) \tag{2}$$

where v_d, v_q, i_d, i_q are the *dq*-axis voltages and currents, respectively; L_d, L_q, R_s are the *dq*-axis inductances as well as the stator resistance, ω_r is the rotor speed, and ψ_m is the rotor PM flux linkage.

It is obvious that, rearranging the *q*-axis (2) it is possible to calculate the rotor flux ψ_m. This would require the measurement of q − axis voltage, stator currents as well as a knowledge of machine parameters R_s, L_d, L_q. Voltage measurements unfortunately are
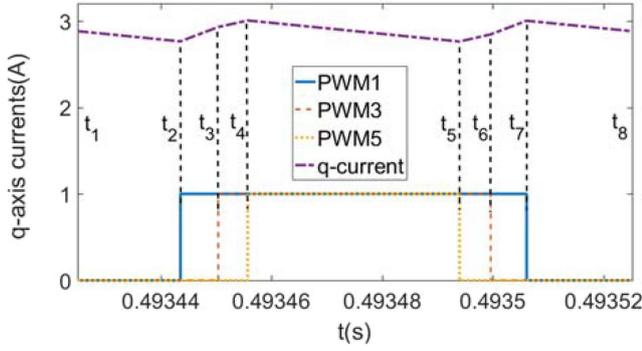
Fig. 1 *Gate signals PWM1, PWM3, PWM5 and the corresponding q-axis current variation in a single switching period*

unavailable in most drive systems as voltage sensors are not commonly installed in motor drives. However, with SV-PWM technique, voltage information can be obtained via the voltage reference vector, the location of which in relation to the active voltage vectors on state vector diagram determines the generation of the PWM switching period [8].

Fig. 1 shows an example of a single PWM switching period with a duration of $t_{switching} = 1/f_{sw}$, where f_{sw} denotes the switching frequency, PWM1,..,3 being the gate signals controlling the turn-on of the top three devices in a standard two-level voltage-source inverter. $t_1 \cdots t_8$ are the time instants at which a different voltage vector is applied. The q-axis (2) can be discretised with a sampling time. $T_s \ll t_{switching}$. The resultant relationships between two adjacent sampling points, assuming the d-axis current to be controlled to zero, are given as:

$$v_{q(t_1 \sim (t_1 + T_s))} = R_s i_{q(t_1 \sim (t_1 + T_s))} + L_q \frac{\mathrm{d}}{\mathrm{d}t} i_{q(t_1 \sim (t_1 + T_s))} + \omega_r \psi_m \quad (3)$$

$$v_{q((t_1 + T_s) \sim (t_1 + 2T_s))} = R_s i_{q((t_1 + T_s) \sim (t_1 + 2T_s))} \\ + L_q \frac{\mathrm{d}}{\mathrm{d}t} i_{q((t_1 + T_s) \sim (t_1 + 2T_s))} + \omega_r \psi_m \quad (4)$$

$$v_{q((t_1 + (n-2)T_s) \sim t_8)} = R_s i_{q((t_1 + (n-2)T_s) \sim t_8)} \\ + L_q \frac{\mathrm{d}}{\mathrm{d}t} i_{q((t_1 + (n-2)T_s) \sim t_8)} + \omega_r \psi_m \quad (5)$$

where T_s is the sampling time, t_1 is the starting point of the PWM period in Fig. 1, and n is the total number of the sampling points in the period, which must be an integer to guarantee an integer number of equations. The speed ω_r is assumed to be constant during the switching period.

The derivative term $\mathrm{d}i_q/\mathrm{d}t$ can be approximated by $i_{q(t_1 + (k+1)T_s)} - i_{q(t_1 + kT_s)}/T_s$, with $k = 0,1 \cdots n - 2$. It is noted that the last sampling point in the period is $t_8 = t_1 + (n-1)T_s$. When the motor operates at steady-state, the current loop controller only responds to the currents measured at the beginning of the non-zero active voltage vectors, which are $i_{q(t_2)}$ and $i_{q(t_5)}$ and ensures that on average they remain constant. This means $i_{q(t_2)} = i_{q(t_5)}$, $i_{q(t_4)} = i_{q(t_7)}$ and also $i_{q(t_1)} = i_{q(t_8)}$. Multiplying the $n - 1$ equations by $\mathrm{d}t$, which is the sampling time T_s gives:

$$T_s v_{q(t_1 \sim (t_1 + T_s))} = T_s R_s i_{q(t_1 \sim (t_1 + T_s))} \\ + L_q (i_{q(t_1 + T_s)} - i_{q(t_1)}) + T_s \omega_r \psi_m \quad (6)$$

$$T_s v_{q((t_1 + T_s) \sim (t_1 + 2T_s))} = T_s R_s i_{q((t_1 + T_s) \sim (t_1 + 2T_s))} \\ + L_q (i_{q(t_1 + 2T_s)} i_{q(t_1 + T_s)}) + T_s \omega_r \psi_m \quad (7)$$

$$T_s v_{q((t_1 + (n-2)T_s) \sim t_8)} = T_s R_s i_{q((t_1 + (n-2)T_s) \sim t_8)} \\ + L_q (i_{q(t_8)} - i_{q(t_1 + (n-2)T_s)}) + T_s \omega_r \psi_m \quad (8)$$

Now adding each equation to the next, it yields:

$$T_s \sum_1^{n-1} v_{q(j)} = T_s R_s \sum_1^{n-1} i_{q(j)} + t_{switching} \omega_r \psi_m \quad (9)$$

where j is the jth equation. It can be noticed that the inductance-related terms are eliminated.

With regard to the voltage terms, it is evident that the sum $\sum_1^{n-1} v_{q(j)}$ measured between two adjacent sampling points is always equivalent to the PWM output voltage:

$$\sum_1^{n-1} v_{q(j)} = (t_3 - t_2) v_{q(t_3 - t_2)} + (t_4 - t_3) v_{q(t_4 - t_3)} \\ + (t_6 - t_5) v_{q(t_6 - t_5)} + (t_7 - t_6) v_{q(t_7 - t_6)}$$

It can be easily verified that:

$$(t_3 - t_2) v_{q(t_3 - t_2)} = (t_7 - t_6) v_{q(t_7 - t_6)}$$

$$(t_4 - t_3) v_{q(t_4 - t_3)} = (t_6 - t_5) v_{q(t_6 - t_5)}$$

as the switching period consists of two symmetrical switching combinations. Therefore, (9) now becomes:

$$2[(t_3 - t_2) v_{q(t_3 - t_2)} + (t_4 - t_3) v_{q(t_4 - t_3)}] = T_s R_s \sum_1^{n-1} i_{q(j)} \\ + t_{switching} \omega_r \psi_m \quad (10)$$

Also, the time differences $(t_3 - t_2)$ and $(t_4 - t_3)$ can be pre-calculated at the beginning of the SVPWM based on the location of the rotating voltage reference vector on the space vector diagram, and $v_{q(t_3 - t_2)}$ and $v_{q(t_4 - t_3)}$ are the results of the switching vectors being transformed from $\alpha\beta$-reference frame to dq-reference frame. In conclusion, the rotor flux can be calculated as:

$$\psi_m = \frac{f_{sw}}{\omega_r} 2[(t_3 - t_2) v_{q(t_3 - t_2)} + (t_4 - t_3) v_{q(t_4 - t_3)}] \\ - \frac{f_{sw}}{\omega_r} T_s R_s \sum_1^{n-1} i_{q(j)} \quad (11)$$

3 Real-time simulation

The proposed methodology has been validated in real-time simulation on a PMSM model with the parameter listed in Table 1. The HIL technique is adopted, which can precisely replicate the dynamics of the physical equipment with computer models running on real-time platforms and, therefore, is an excellent replacement to the expensive conventional testing. Fig. 2 describes the HIL implementation, in which machine and power converter are simulated on the National Instrument (NI) myRIO-1900 data acquisition and control platform. The real-time modelling has been validated in [9]. A standard field-oriented motor control with SV-PWM along with the proposed flux estimation is implemented in the OPAL-RT 5600 platform.
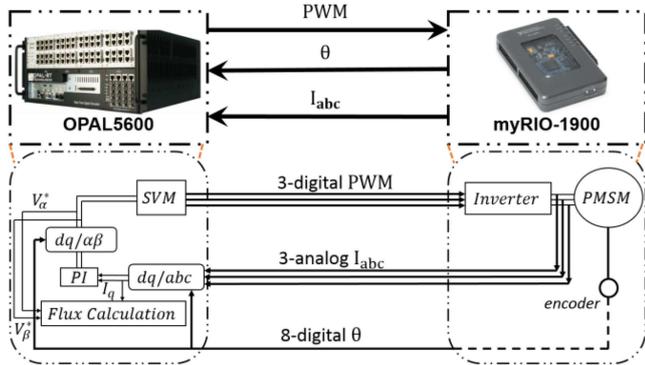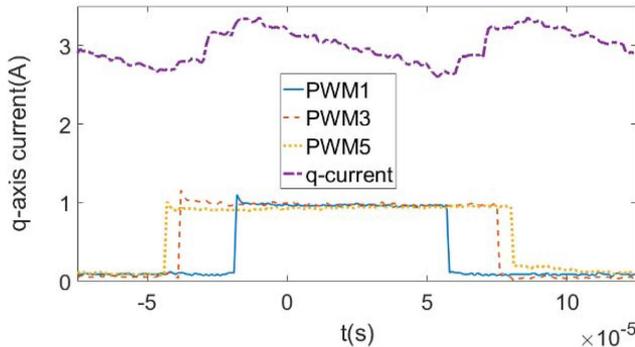
3.1 Steady-state test

The theory upon which the presented method is based is tested in real-time simulation. Fig. 3 shows the measured q-axis current variation and the three PWM signals from the SV-PWM. It can be seen that in steady-state conditions, the currents at the beginning of the non-zero voltage periods are always identical, due to PI controller regulating the average q-axis current.

Fig. 4 depicts the estimated flux linkage when the machine operates at the rated torque and a relatively high speed (1000 rpm) at room temperature. It can be observed that the estimated flux linkage is ~0.1096 Wb, corresponding to − 2.23% estimation error with respect to the reference value.

Fig. 5 shows the flux linkage estimation under the operating conditions that the torque (current) and room temperature remain

2

Table 1 Parameters for the tested IPMSM [10]

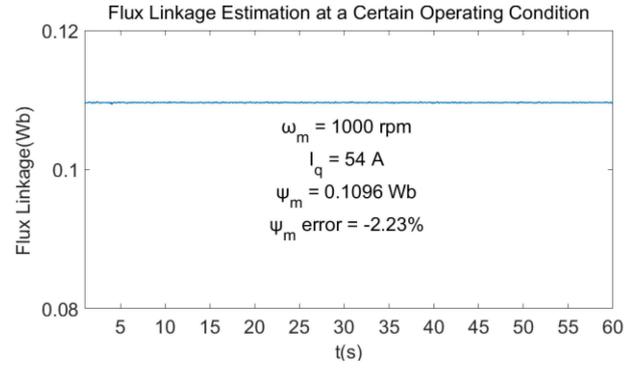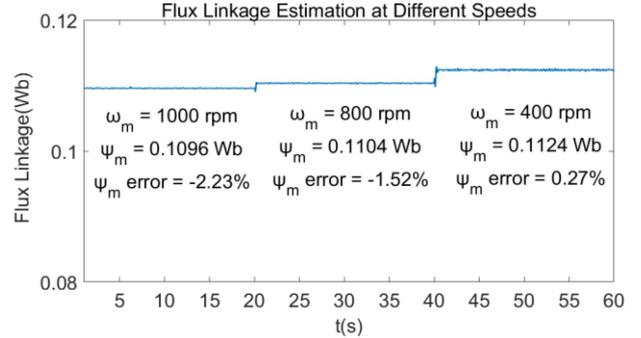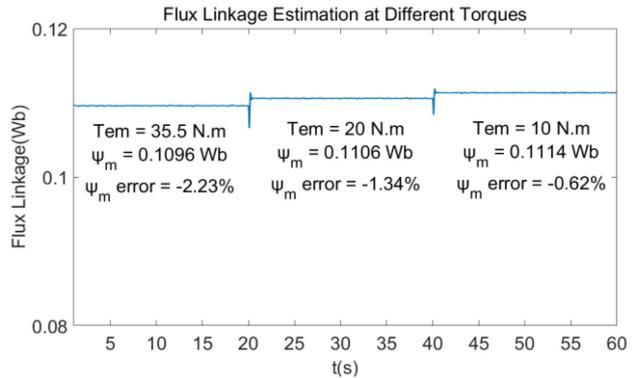| Quantity	Unit	Value
peak torque	Nm	70
rated torque	Nm	35.5
base speed	r/min	1350
max speed	r/min	4500
peak power	kW	9.9
rated power	kW	5
DC link voltage	V	120
peak current	A	125
no. of pole-pairs	—	3
no. of slots	—	36
active stack length	mm	118
stator outer diameter	mm	150
rotor outer diameter	mm	80
stator resistance	Ω	0.0545
d-axis Inductance	mH	0.8258
q-axis Inductance	mH	1.8711
PM flux linkage	Wb	0.1121

Fig. 2 *HIL implementation scheme*

Fig. 3 *PWM1, PWM3, PWM5 and the corresponding q-axis current variation within one switching period in real-time simulation*

unchanged while a 800 and a 400 rpm speeds are applied at $t = 20$ s and $t = 40$ s, respectively. In comparison with the reference value, the flux linkage exhibits a -1.52% and $+0.27\%$ errors at these speeds. Fig. 6 illustrates the result with two different values of load torque (20Nm and 10Nm) being imposed at $t = 20$ and $t = 40$ s, in which a -1.34% and -0.62% deviations are observed.

The slight difference in flux linkage estimation at different conditions is mainly due to the fact that the calculation uses reference voltages which are slightly different from the voltages applied to the motor due to small inaccuracy in the real-time emulations. Furthermore, a triggering signal is needed to define the starting point of each switching period. Here, an additional PWM with its duty cycle close to 0 is employed for this propose. By triggering either the rising, or the falling edge of this PWM, the absolutely starting point, as t_1 in Fig. 1, can be roughly located. An

Fig. 4 *Flux linkage estimation at a specific operating condition*

Fig. 5 *Flux linkage estimations at 1000 rpm, 800 and 400 rpm machine rotating speeds*

Fig. 6 *Flux linkage estimations at 35.5N.m, 20N.m and 10N.m machine electromechanical torques*

error in voltage always exists due to small delays in the triggering of the current acquisition.

Furthermore, the current used for the flux linkage calculation is acquired from the machine model and is acquired by the control unit with a sampling time of 10 μs, which is relatively large due to the requirement of completing relatively complex calculations (11) and the standard FOC algorithm within one sampling step. A practical switching frequency of 5 kHz for SV-PWM is employed. The usage of 10 μs ensures the number of the sampling points, and thus the number of the equations, in a switching period is integer.

With the relatively big 10 μs sampling time, some error in the ability to correctly capture variable voltages and currents is inevitable. However, the effect on the precision of the method is relatively modest.

3.2 Transient test

A three-node LPTN consisting of the stator iron, stator winding and PM nodes, as illustrated in Fig. 7 has been used for thermal evaluation in the real-time simulations. The thermal resistance $R_W$$_{-Fes}$ takes into consideration the heat conduction effect through solid components of PMSM, and heat convection through ambient, air gap, and cooling system is described by R_{PM-A}, R_{PM-Fes}, R_{PM}
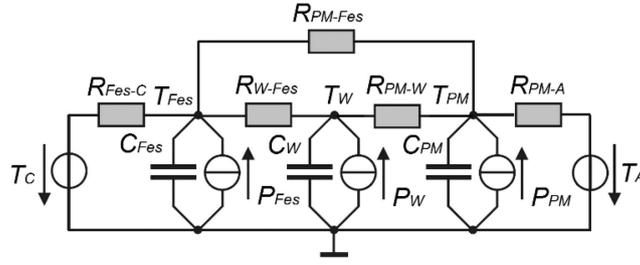
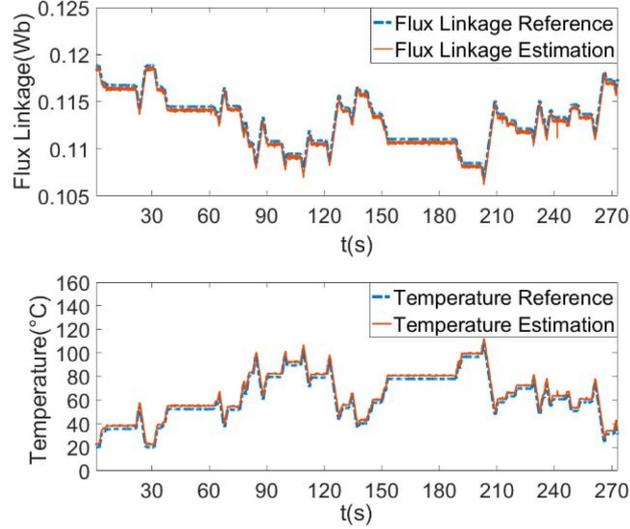**Fig. 7** *Schematic graph of the three-node LPTN*

Fig. 8 *Flux linkage (top) and rotor temperature (bottom) estimations at the rated torque and 500 rpm rotating speed conditions according to the test driving cycle used on the single-node thermal network*
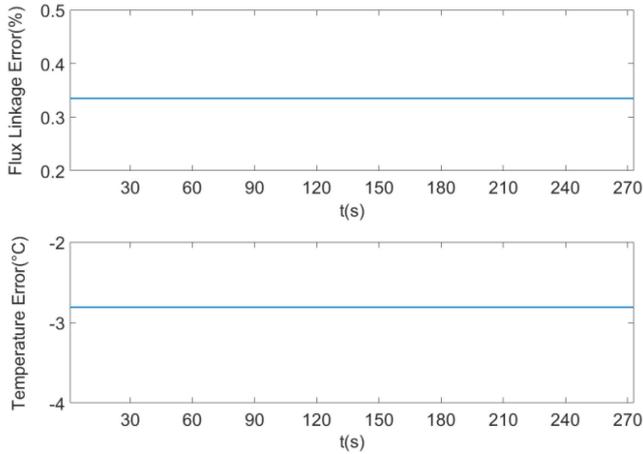

Fig. 9 *Flux linkage (top) and rotor temperature (bottom) estimation errors for the test in Fig. 8*

Fig. 10 *Load profile*

$-W$ as well as R_{Fes}–c, respectively. P_W is the copper loss calculated by $P_w = I^2R$, while speed-dependent iron loss is approximated by the sum of P_{OC} and P_{SC} in (12) and (13) and is allocated into stator iron and PM nodes according to the proportion of iron utilised in stator and rotor [11].

$$P_{\text{OC}} = a_h f + a_J f^2 + a_{\text{ex}} f^{1.5} \qquad (12)$$

$$P_{\text{SC}} = b_h f + b_J f^2 + b_{\text{ex}} f^{1.5} \qquad (13)$$

where P_{OC} and P_{SC} are the losses for open-circuit and short-circuit conditions, respectively. The iron loss is parted into hysteresis, eddy current, and excess loss components, and the corresponding coefficients can be calculated by finite element analyses (FEA) at open-circuit and short-circuit operations, with a single random
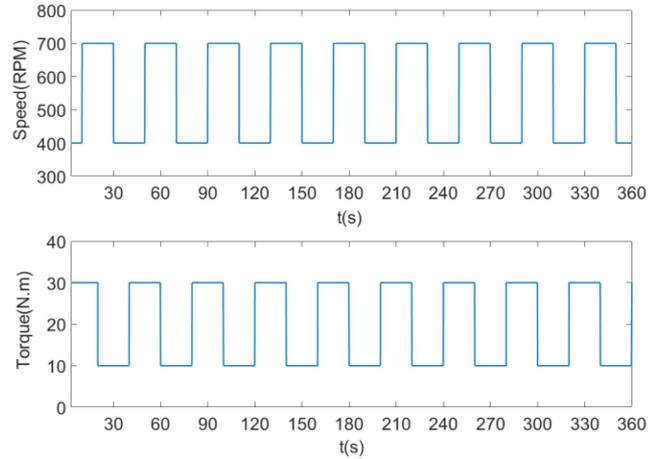
frequency f applied. The flux linkage is assumed to be linearly dependent on temperature as:

$$\psi_m(T) = \psi_m(T_{\text{ref}})\left[1 + \alpha_{\beta r}(T - T_{\text{ref}})\right] \qquad (14)$$

where $\psi_m(T)$ and $\psi_m(T_{\text{ref}})$ are the flux linkages at the rotor and reference temperatures (70°C); $\alpha_{\beta r}$ is a temperature-dependent coefficient, which for NeFeB magnet is $\sim -0.12\%/°C$.

A thermal transient case is considered where the machine is controlled at the rated torque and at a speed of 500 rpm. Excellent result from the proposed method is shown in Fig. 8, accompanied by the corresponding rotor temperature variation. An error of $\sim +0.3\%$ in flux linkage and $-3°C$ in rotor temperature is demonstrated in Fig. 9.

In order to validate the proposed method in non-stationary conditions, a simplified duty cycle with step variations in speed and torque as plotted in Fig. 10 is considered.
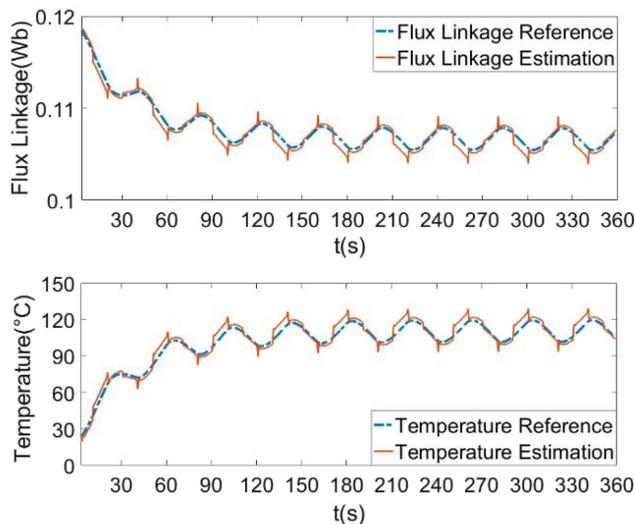
Fig. 11 *Flux linkage (top) and rotor temperature (bottom) estimations according to the test driving cycle used on the simplified three-nodes thermal network*
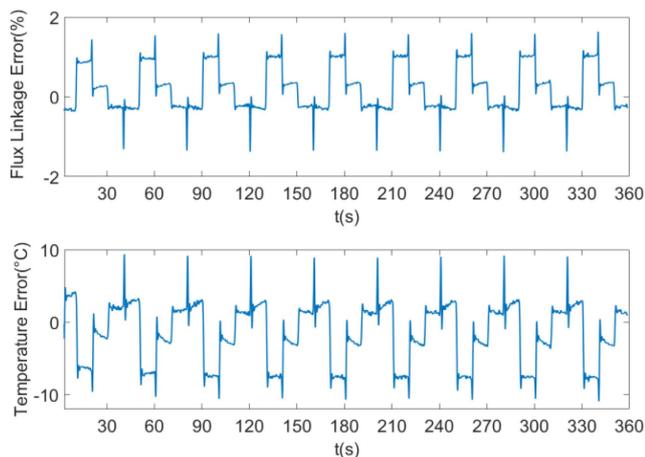

Fig. 12 *Flux linkage (top) and rotor temperature (bottom) estimation errors in Fig. 11*

As it can be seen from Figs. 11 and 12, $< \pm 2\%$ errors in flux linkage estimation are obtained, and all estimated rotor temperatures lie within an $\sim \pm 10°C$ band around their corresponding reference values. Unfortunately, a very small error in the flux linkage estimation is amplified in the estimation of temperature due to the very small temperature coefficient $\alpha_{\beta r}$. Nevertheless, the error in the temperature estimation is contained within $\pm 9\%$. Some dependency on the operating conditions (speed, current) is apparent. This is due to the relatively slow acquisition of

10 μs, which creates small error in the timing and current/voltage measurement that change with a variable modulation index. It is expected that these effects can be minimised with a faster acquisition unit.

4 Conclusion

This paper introduces a relatively simple and accurate method for online flux linkage estimation of PMSMs, based on the current response to the standard SV-PWM which is commonly employed in most state-of-the-art power converter drive applications. This method is simple to implement and does not require additional hardware neither create additional disturbance to the machine as no additional signal injection is required. The method is also independent of machine inductances. A series of real-time simulations have been presented to validate the presented methodology on a typical IPMSM, utilising the HIL technique. The experimental results demonstrate good accuracy in rotor flux linkages and temperature estimation in a wide range of machine operating conditions. Further experimental validations and improvement to the signal acquisition and processing will be explored in future research.

5 References

[1]   Huber, T., Peters, W., Bocker, J.: 'A low-order thermal model for monitoring critical temperatures in permanent magnet synchronous motors'. Proc. IEEE Int. Conf. PEMD, Manchester, UK, October 2014, pp. 1–6
[2]   Specht, A., Bocker, J.: 'Observer for the rotor temperature of IPMSM'. Proc. 14th Int. Power Electronics and Motion Control Conf. (EPE/PEMC), Ohrid, Macedonia, September 2010, pp. T4-12–T4-15
[3]   Wallscheid, O., Bocker, J.: 'Fusion of direct and indirect temperature estimation techniques for permanent magnet synchronous motors'. IEEE Int. Electric Machines and Drives Conf. (IEMDC), Miami, FL, USA, August 2017
[4]   Wallscheid, O., Bocker, J.: 'Global identification of a low-order lumped-parameter thermal network for permanent magnet synchronous motors', *IEEE Trans. Energy Convers.*, 2016, **31**, (1), pp. 354–365
[5]   Wallscheid, O., Specht, A., Bocker, J.: 'Observing the permanent temperature of synchronous motors based on electrical fundamental wave model quantites', *IEEE Trans. Ind. Electron.*, 2017, **64**, pp. 3921–3929
[6]   Liu, K., Zhu, Z., Stone, D.: 'Parameter estimation for condition monitoring of PMSM stator winding and rotor permanent magnets', *IEEE trans. Ind. Electron.*, 2013, **60**, (12), pp. 5902–5913
[7]   Xie, G., Lu, K., Dwivedi, S.K*., et al.*: 'Permanent magnet flux online estimation based on zero-voltage vector injection method', *IEEE Trans. Power Electron.*, 2015, **30**, (12), pp. 6506–6509
[8]   Bose, B.K.: '*Modern power electronics and AC drives*' (Prentice Hall PTR, Upper Saddle River, NJ, 2002)
[9]   Gonzalez, F.A., Griffo, A., Sen, B*., et al.*: 'Real-time hardware-in-the-loop simulation of permanent magnet synchronous motor drives under stator faults', *IEEE Trans. Ind. Electron.*, 2017, **64**, (9), pp. 6960–6969
[10]   Chen, X., Wang, J., Sen, B*., et al.*: 'A high-fidelity, computationally efficient model for interior permanent magnet machines considering the magnetic saturation, spatial harmonics and iron loss effect', *IEEE Trans. Ind. Electron.*, 2015, **62**, (7), pp. 4044–4055
[11]   Mellor, P.H., Wrobel, R.: 'A computationally efficient iron loss model for brushless AC machines that caters for rated flux and field weakened operation'. IEEE Int. Electric Machines and Drives Conf. (IEMDC), May 2009, pp. 490–494